J. Fluid Mech. (2010), *vol.* 656, *pp.* 223–230. © Cambridge University Press 2010
doi:10.1017/S0022112010001771

Echoing in a viscous compressible fluid confined between two parallel plane walls

B. U. FELDERHOF†

Institut für Theoretische Physik A, RWTH Aachen, Templergraben 55, 52056 Aachen, Germany

(Received 1 February 2010; revised 1 April 2010; accepted 2 April 2010;
first published online 1 July 2010)

The dynamics of a viscous compressible fluid, confined between two parallel plane walls and excited by a sudden impulse transverse to the walls, is studied on the basis of the linearized Navier–Stokes equations. It is shown that the time-dependent flow depends strongly on the sound velocity and on the shear and volume viscosity. Under favourable conditions an echoing effect can be observed, with a sound pulse bouncing many times between the two plates. The velocity correlation function of a Brownian particle immersed in the fluid is calculated in point approximation. It shows a similar strong dependence on fluid properties.

Key words: channel flow, low-Reynolds-number flows, micro-/nano-fluid dynamics

1. Introduction

The study of the dynamics of fluids confined to a small length scale is relevant in microfluidics and biophysics. Brownian motion of a particle suspended in a fluid is governed by hydrodynamic fluctuations which are affected by the geometry. It has been argued by Hagen *et al.* (1997) and Pagonabarraga *et al.* (1999) on the basis of mode-coupling theory that for a fluid confined between two flat walls the velocity correlation function for motion parallel to the walls decays with a negative t^{-2} long-time tail due to coupling to overdamped sound waves. Frydel & Rice (2006) showed in a lattice-Boltzmann simulation that for motion perpendicular to the walls the velocity correlation function shows oscillating behaviour due to reflection of sound waves between the two walls. Later they showed similar behaviour for the Green function of the linearized Navier–Stokes equations for a fluid satisfying perfect slip boundary conditions at the walls (Frydel & Rice 2007). In both simulations and theory the oscillations occur in a regime where the velocity correlation function and the Green function are positive.

In an earlier work (Felderhof 2006), we have provided an analytic expression for the Green function and the velocity correlation function of a Brownian particle for a compressible fluid confined between two parallel plane walls and satisfying the no-slip boundary condition at the walls. We showed in numerical examples that the correlation function for motion perpendicular to the walls rapidly turns negative before decaying in oscillatory manner. This behaviour differs qualitatively from that found by Frydel & Rice (2006). In the following we analyse the theory in more detail and show that a wide variety of behaviour is possible, depending on the velocity

† Email address for correspondence: ufelder@physik.rwth-aachen.de

https://doi.org/10.1017/S0022112010001771 Published online by Cambridge University Press

of sound, the shear and bulk viscosity of the fluid, and the mass and size of the Brownian particle.

Under suitable conditions a persistent echoing effect can be observed in which a sound pulse is reflected many times between the two walls. The strength of the echoing effect can be estimated from a spectral function related to the Green function. A conspicuous echo is signalled by a strong peak in the spectral function.

2. Linear hydrodynamics

We consider a spherical particle of radius a and mass m_p, immersed in a viscous compressible fluid of shear viscosity η, bulk viscosity η_v and equilibrium mass density ρ_0. The sphere and the fluid are confined between two parallel plates located at $z=0$ and $z=L$. The fluid is assumed to satisfy no-slip boundary conditions at the two plates and at the surface of the sphere. The centre of the particle performs small motions about the rest position $\boldsymbol{r}_0$. In Cartesian coordinates $\boldsymbol{r}_0=(0,0,h)$ with height h satisfying $h>a$ and $h\leqslant L/2$.

For small-amplitude motion the flow velocity $\boldsymbol{v}(\boldsymbol{r},t)$ and the pressure $p(\boldsymbol{r},t)$ are governed by the linearized Navier–Stokes equations (Acheson 1990):

$$\left.\begin{aligned}\rho_0\frac{\partial \boldsymbol{v}}{\partial t}&=\eta\nabla^2\boldsymbol{v}+\left(\frac{1}{3}\eta+\eta_v\right)\nabla\nabla\cdot\boldsymbol{v}-\nabla p,\\ \frac{\partial p}{\partial t}&=-\rho_0c_0^2\nabla\cdot\boldsymbol{v},\end{aligned}\right\}\tag{2.1}$$

where c_0 is the long-wave sound velocity. After Fourier analysis in time we find that the equations for the Fourier components with time-factor $\exp(-\mathrm{i}\omega t)$ are

$$\left.\begin{aligned}\eta(\nabla^2\boldsymbol{v}_\omega-\alpha^2\boldsymbol{v}_\omega)+\left(\frac{1}{3}\eta+\eta_v\right)\nabla\nabla\cdot\boldsymbol{v}_\omega-\nabla p_\omega&=0,\\ \nabla\cdot\boldsymbol{v}_\omega-i\beta p_\omega&=0,\end{aligned}\right\}\tag{2.2}$$

where we have used the abbreviations

$$\alpha=(-\mathrm{i}\omega\rho_0/\eta)^{1/2},\qquad \mathrm{Re}\,\alpha>0,\qquad \beta=\frac{\omega}{\rho_0c_0^2}.\tag{2.3}$$

The motion of the particle is determined by the applied force $\boldsymbol{E}(t)$, the force $\boldsymbol{K}(t)$ exerted by the fluid and by its mass. The force exerted by the fluid depends linearly on the applied force via the Navier–Stokes equations (2.1) and the boundary conditions. Therefore the particle velocity $\boldsymbol{U}(t)$ depends linearly on the applied force. In Fourier language the relation is expressed by

$$\boldsymbol{U}_\omega=\mathscr{Y}(\boldsymbol{r}_0,\omega)\cdot\boldsymbol{E}_\omega\tag{2.4}$$

with admittance tensor

$$\mathscr{Y}(\boldsymbol{r}_0,\omega)=\mathscr{Y}_0(\omega)[\mathbf{1}+A(\omega)C(\omega)\boldsymbol{F}_a(\boldsymbol{r}_0,\omega)],\tag{2.5}$$

where $\mathscr{Y}_0(\omega)$ is the scalar admittance for infinite space,

$$\mathscr{Y}_0(\omega)=[-\mathrm{i}\omega m_p+\zeta(\omega)]^{-1},\tag{2.6}$$

with friction coefficient $\zeta(\omega)$. The coefficient $A(\omega)$ is given by a simple quadratic expression in terms of the variable αa, and is independent of sound velocity and bulk viscosity. The coefficient $C(\omega)$ is more complicated, and does depend on sound velocity and bulk viscosity. The explicit expressions (Bedeaux & Mazur 1974) have

https://doi.org/10.1017/S0022112010001771 Published online by Cambridge University Press

been given in Felderhof (2005*b*). In the present situation the reaction field tensor $\boldsymbol{F}_a(\boldsymbol{r}_0, \omega)$ is diagonal by symmetry in the chosen system of coordinates, and the xx and yy components are equal.

In point approximation, the reaction field tensor is given by

$$\boldsymbol{F}(\boldsymbol{r}_0, \omega) = \lim_{\boldsymbol{r}\to\boldsymbol{r}_0} (\boldsymbol{G}(\boldsymbol{r}, \boldsymbol{r}_0) - \boldsymbol{G}_0(\boldsymbol{r} - \boldsymbol{r}_0)), \tag{2.7}$$

where $\boldsymbol{G}(\boldsymbol{r}, \boldsymbol{r}_0)$ is the Green function for the linearized Navier–Stokes equations for the present two-wall geometry in the absence of the sphere, and $\boldsymbol{G}_0(\boldsymbol{r}-\boldsymbol{r}_0)$ is the Green function for infinite space. The latter Green function is translationally invariant, and given by a fairly simple expression. The Green function $\boldsymbol{G}(\boldsymbol{r}, \boldsymbol{r}_0)$ has been calculated elsewhere (Felderhof 2006), and is quite complicated. In the following we consider, in particular, the zz component of the reaction field tensor (2.7) corresponding to the z component of velocity in response to a force applied in the z direction.

We write the zz element of the reaction field tensor in the form

$$F_{zz}(h, L, \omega) = \frac{1}{4\pi\eta h} Z(h, L, \omega) \tag{2.8}$$

with dimensionless function $Z(h, L, \omega)$. The latter is found as an integral over wavenumber q arising from the Fourier transform in the x and y directions,

$$Z(h, L, \omega) = h \int_0^\infty f_z(q, \omega) q \, \mathrm{d}q. \tag{2.9}$$

The integrand $f_z(q, \omega)$ is expressed conveniently as a function of the variables

$$r = \sqrt{q^2 - \mu^2}, \qquad s = \sqrt{q^2 + \alpha^2}. \tag{2.10}$$

We have used the abbreviation

$$\mu = \omega/c, \qquad \mathrm{Im}\mu > 0, \tag{2.11}$$

where

$$c = c_0 \left[1 - \mathrm{i}\beta \left(\frac{4}{3}\eta + \eta_v\right)\right]^{1/2} \tag{2.12}$$

is the frequency-dependent sound velocity.

The integrand in (2.9) can be written as the fraction

$$f_z(q, \omega) = \frac{N_z(q, \omega)}{D_z(q, \omega)}. \tag{2.13}$$

We give here only the expressions for the case where the particle is located midway between the two planes, corresponding to $h = L/2$, and refer for the expressions for the general case to Felderhof (2006). We introduce the abbreviations

$$n = \exp[rL/2], \qquad u = \exp[sL/2]. \tag{2.14}$$

In terms of these variables the numerator $N_z(q, \omega)$ is given by

$$\begin{aligned} N_z(q, \omega) = 2[&-(q^2 - rs)^3 + q^2(q^4 - r^2s^2)u^2 - rs(q^2 + rs)^2u^4 - 4q^2rsu[q^2 - rs - (q^2 \\ &+ rs)u^2]n + rs(q^2 - rs)[q^2 + rs - 4q^2u^2 - (q^2 + rs)u^4]n^2 - 4q^2rsu[q^2 \\ &+ rs - (q^2 - rs)u^2]n^3 + q^2(q^2 + rs)[q^2 + rs - (q^2 - rs)u^2]n^4]. \end{aligned} \tag{2.15}$$

The denominator $D_z(q, \omega)$ is given by

$$D_z(q, \omega) = s(q^2 - s^2)[(q^2 - rs)^2(1 + u^4n^4) + 8q^2rsu^2n^2 - (q^2 + rs)^2(u^4 + n^4)]. \tag{2.16}$$

The expressions take account of the multiple reflection of waves at the two walls.

https://doi.org/10.1017/S0022112010001771 Published online by Cambridge University Press

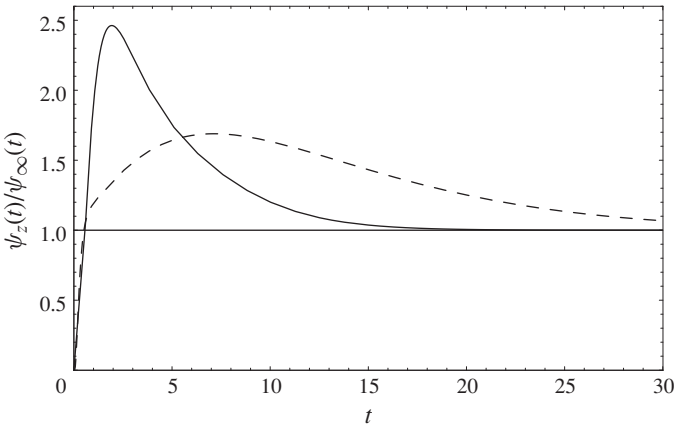


FIGURE 1. Plot of the $\psi_z(t)/\psi_\infty(t)$ for the case $(c_0, \eta_v) = (1, 0)$ (solid curve) and the case $(c_0, \eta_v) = (1, 3)$ (dashed curve).

3. Reaction flow and velocity autocorrelation function

The reaction factor $F_{zz}(\mathbf{0}, \omega)$ may be regarded as the Fourier transform of a function $\psi_z(t)$ according to

$$F_{zz}(\mathbf{0}, \omega) = \frac{1}{6\pi\rho_0 h^3} \int_0^\infty e^{i\omega t} \psi_z(t)\, dt. \tag{3.1}$$

The dimensionless function $\psi_z(t)$ may be calculated by inverse Fourier transform of the expressions derived in the preceding section. The function starts at zero, since the sound wave needs a finite time to be reflected from the walls of the duct. The asymptotic behaviour at long times of the corresponding function for an incompressible fluid and a single wall at distance h from the source point is given by (Felderhof 2005*a*)

$$\psi_\infty(t) = \frac{-1}{2\sqrt{\pi}} \tau^{-3/2}, \tag{3.2}$$

where $\tau = t/\tau_w$ with $\tau_w = h^2\rho_0/\eta$. The behaviour is due to the second term in (2.7). The asymptotic analysis in Felderhof (2006) shows that the function $\psi_z(t)$ for the duct has the same long-time behaviour.

It is convenient to choose the unit of length such that $L = 2$. We have chosen the source point midway between the two planes, so that $h = 1$. Furthermore, we choose the unit of mass such that $\rho_0 = 1$, and the unit of time such that $\eta = 1$. Then the only free parameters are the velocity of sound c_0 and the volume viscosity η_v. We consider two values for the sound velocity: $c_0 = 1$ corresponding to a very compressible fluid, and $c_0 = 20$, corresponding to a less compressible fluid. We also consider two values for the volume viscosity: $\eta_v = 0$, corresponding to a dilute monatomic gas, and $\eta_v = 3$, corresponding to the ratio $\eta_v/\eta = 3.09$ for water. In the simulation of Frydel & Rice (2006), the ratio of volume viscosity to shear viscosity takes the value $\eta_v/\eta = 2/3$. In lattice-Boltzmann simulation the ratio η_v/η can be varied continuously from 0 to a large positive value (Dellar 2001).

For the four cases we calculate the function $\psi_z(t)$ numerically, and compare with the function $\psi_\infty(t)$ given by (3.2). In figure 1 we show the ratio $\psi_z(t)/\psi_\infty(t)$ for the cases $(c_0, \eta_v) = (1, 0)$ and $(c_0, \eta_v) = (1, 3)$, and in figure 2 we show the ratio $\psi_z(t)/\psi_\infty(t)$ for the cases $(c_0, \eta_v) = (20, 0)$ and $(c_0, \eta_v) = (20, 3)$. In the case $(c_0, \eta_v) = (20, 0)$ the function

https://doi.org/10.1017/S0022112010001771 Published online by Cambridge University Press

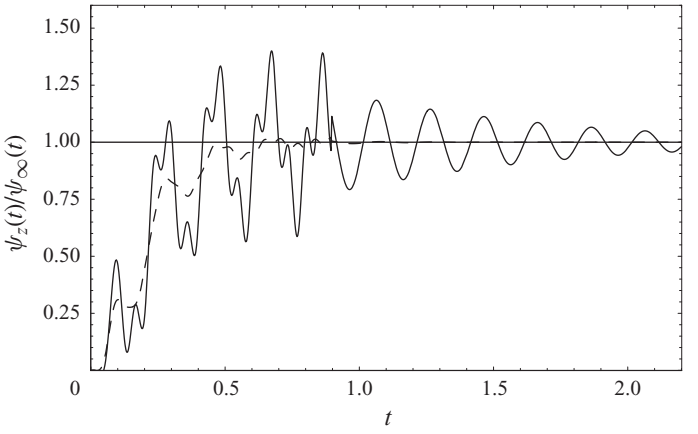


FIGURE 2. Plot of the ratio $\psi_z(t)/\psi_\infty(t)$ for the case $(c_0, \eta_v) = (20, 0)$ (solid curve) and the case $(c_0, \eta_v) = (20, 3)$ (dashed curve).

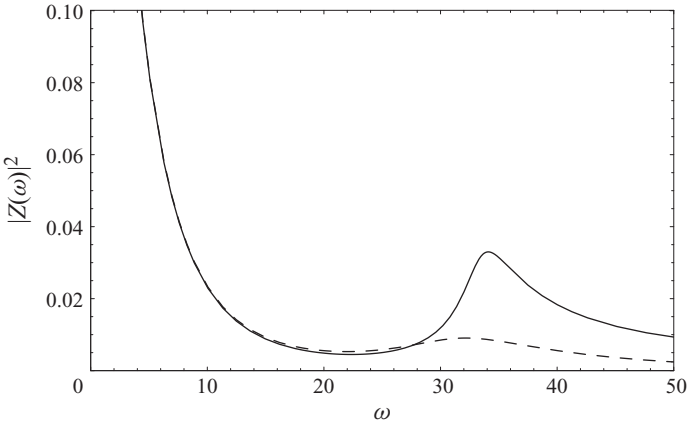


FIGURE 3. Plot of the spectral function $|Z(1, 2, \omega)|^2$ as a function of frequency ω for the case $(c_0, \eta_v) = (20, 0)$ (solid curve) and the case $(c_0, \eta_v) = (20, 3)$ (dashed curve).

shows damped oscillations with a period of approximately $T_0 = 2L/c_0$ corresponding to reflection of the sound pulse, generated by the initial impulse, between the two walls.

The echoing effect shown in figure 2 is due to the excitation of sound waves which travel nearly perpendicularly to the two walls. Due to the kinematic boundary condition at $z = 0$ and $z = L$ the z component of the wave vector of planar sound waves can take only discrete values $j\pi/L$ with integer j. In the lowest mode the z component of velocity must be proportional to $\sin \pi z/L$, corresponding to $j = 1$. Hence we expect a resonance in the function $f_z(q, \omega)$ for small q near $\omega_0 = 2\pi/T_0 = \pi c_0/L$.

Numerical investigation of the function $Z(1, 2, \omega)$ shows very complicated behaviour in the lower half of the complex frequency plane. On the real axis the absolute value of the function shows a peak near ω_0, and for sufficiently small dissipation also peaks near $\omega_j = j\,\omega_0$ with j odd. In figure 3 we show the behaviour of $|Z(1, 2, \omega)|^2$ for the cases $(c_0, \eta_v) = (20, 0)$ and $(c_0, \eta_v) = (20, 3)$. In the first case, there is a pronounced peak near ω_0. The peak is still visible for $\eta_v = 3$, but is much lower and wider. The strong peak near $\omega = 0$ corresponds to coupling to viscous

https://doi.org/10.1017/S0022112010001771 Published online by Cambridge University Press

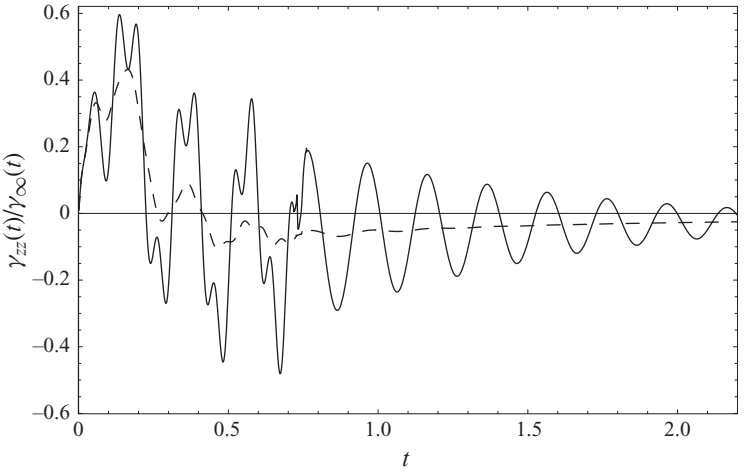


FIGURE 4. Plot of the ratio $\gamma_{zz}(t)/\gamma_\infty(t)$ for the case $(c_0, \eta_v) = (20, 0)$ (solid curve) and the case $(c_0, \eta_v) = (20, 3)$ (dashed curve).

shear modes. The value at $\omega = 0$ is $|Z(1, 2, 0)|^2 = Z_0(1/2)^2 = 0.9365$ independent of the parameters (Felderhof 2006). A Padé approximant analysis confirms the asymptotic behaviour of the function $\psi_z(t)$ given by (3.2).

In experiment or computer simulation, the velocity autocorrelation function of a Brownian particle immersed in the fluid can be measured. We consider here, in particular, the function

$$C_{zz}(t) = \langle U_z(t) U_z(0) \rangle, \tag{3.3}$$

where the angle brackets denote the equilibrium ensemble average at absolute temperature T. According to the fluctuation-dissipation theorem the Fourier transform of $C_{zz}(t)$ is given by

$$\hat{C}_{zz}(\omega) = \int_0^\infty \mathrm{e}^{\mathrm{i}\omega t} C_{zz}(t)\, \mathrm{d}t = k_B T \mathscr{Y}_{zz}(0, \omega), \tag{3.4}$$

where k_B is Boltzmann's constant. By substitution of $F_{zz}(0, \omega)$ into (2.5) we may calculate the function $C_{zz}(t)$ numerically by inverse Fourier transform. It is convenient to consider the normalized function

$$\gamma_{zz}(t) = \frac{m_p}{k_B T} C_{zz}(t) \tag{3.5}$$

with initial value $\gamma_{zz}(0) = 1$. We compare the function $\gamma_{zz}(t)$ with the long-time tail which it would have in infinite space, given by

$$\gamma_\infty(t) = \frac{m_p}{12(\pi \nu t)^{3/2}}, \tag{3.6}$$

where $\nu = \eta/\rho_0$ is the kinematic shear viscosity. In figure 4 we show the ratio $\gamma_{zz}(t)/\gamma_\infty(t)$ for the case $(c_0, \eta_v) = (20, 0)$ and a neutrally buoyant Brownian particle of radius $a = 1/3$. We show the ratio of the two functions in order to amplify the long-time behaviour. At the last minimum shown, the function $\gamma_{zz}(t)$ takes the value $\gamma_{zz}(2.06) = -6 \times 10^{-5}$. The coupling to the sound modes again gives rise to an echoing effect. The long-time behaviour of the function $\psi_z(t)$, given by (3.2), is precisely such as to cancel the $t^{-3/2}$ long-time tail of the velocity correlation

https://doi.org/10.1017/S0022112010001771 Published online by Cambridge University Press

function in bulk fluid, as follows from (2.5). The presence of the walls causes a faster decay.

The echoing effect has been seen in the computer simulation of Frydel & Rice (2006), both for no-slip and perfect slip boundary conditions at the walls. Apparently, the value of the sound velocity c_s used in Frydel & Rice (2007, figure 5) equals approximately $c_0/2$. The behaviour of the function $\gamma_{zz}(t)$ was shown for two other numerical examples in Felderhof (2006, figures 5, 6 and 8), corresponding to fluids of effectively larger compressibility (in figure 8 the function $\gamma_{zz}(t)$ is shown, rather than $\gamma_{xx}(t)$, as indicated erroneously in the same paper).

4. Discussion

We have shown that the flow of a viscous compressible fluid confined between two parallel plane walls depends strongly on sound velocity and viscosity coefficients. If the fluid is excited by an impulse transverse to the walls, an echoing effect can be seen with a sound pulse bouncing many times between the two walls, provided the fluid is sufficiently incompressible, and correspondingly has a large sound velocity c_0. The period of oscillation is $T_0 = 2L/c_0$, and this must be short in comparison with the viscous relaxation time $L^2\rho_0/\eta$. For too small sound velocity, the velocity correlation function has decayed before significant echoing can be seen. The presence of echoing behaviour is signalled by a peak in the spectral function $|Z(h, L, \omega)|^2$ near the frequency $\omega_0 = \pi c_0/L$. The flow is strongly affected by the ratio of volume to shear viscosity η_v/η. Large volume viscosity leads to additional dissipation and may suppress the echoing.

The analysis demonstrates that in fluid flow on a small length scale it is important to take fluid compressibility into account. Besides the sound velocity, both shear viscosity and volume viscosity must be known accurately in order to allow prediction of the flow behaviour. The relevance of fluid compressibility to gas flow through a microchannel has been discussed by Gat, Frankel & Weihs (2008, 2009).

The Green function is intimately related to the correlation function of thermal velocity fluctuations in the fluid (Felderhof 2006). This suggests that the echoing effect can be seen in a light scattering experiment.

REFERENCES

Acheson, D. J. 1990 *Elementary Fluid Dynamics*. Clarendon Press.

Bedeaux, D. & Mazur, P. 1974 A generalization of Faxen's theorem to nonsteady motion of a sphere through a compressible fluid in arbitrary flow. *Physica* A **78**, 505.

Dellar, P. J. 2001 Bulk and shear viscosities in lattice Boltzmann equations. *Phys. Rev.* E **64**, 031203.

Felderhof, B. U. 2005*a* Effect of the wall on the velocity autocorrelation function and long-time tail of Brownian motion. *J. Phys. Chem.* B **109**, 21406.

Felderhof, B. U. 2005*b* Effect of the wall on the velocity autocorrelation function and long-time tail of Brownian motion in a viscous compressible fluid. *J. Chem. Phys.* **123**, 184903.

Felderhof, B. U. 2006 Diffusion and velocity relaxation of a Brownian particle immersed in a viscous compressible fluid confined between two parallel plane walls. *J. Chem. Phys.* **124**, 054111.

Frydel, D. & Rice, S. A. 2006 Lattice Boltzmann study of the transition from quasi-two-dimensional to three-dimensional one particle hydrodynamics. *Mol. Phys.* **104**, 1283.

Frydel, D. & Rice, S. A. 2007 Hydrodynamic description of the long-time tails of the linear and rotational velocity autocorrelation functions of a particle in a confined geometry. *Phys. Rev.* E **76**, 061404.

https://doi.org/10.1017/S0022112010001771 Published online by Cambridge University Press

Gat, A. D., Frankel, I. & Weihs, D. 2008 Gas flows through constricted shallow micro-channels. *J. Fluid Mech.* **602**, 427.

Gat, A. D., Frankel, I. & Weihs, D. 2009 A higher-order Hele-Shaw approximation with application to gas flows through shallow micro-channels. *J. Fluid Mech.* **638**, 141.

Hagen, M. H. J., Pagonabarraga, I., Lowe, C. P. & Frenkel, D. 1997 Algebraic decay of velocity fluctuations in a confined fluid. *Phys. Rev. Lett.* **78**, 3785.

Pagonabarraga, I., Hagen, M. H. J., Lowe, C. P. & Frenkel, D. 1999 Short-time dynamics of colloidal suspensions in confined geometries. *Phys. Rev.* E **59**, 4458.

https://doi.org/10.1017/S0022112010001771 Published online by Cambridge University Press